HHS Public Access

Author manuscript

Extracell Vesicle. Author manuscript; available in PMC 2024 April 25.

Published in final edited form as:

Extracell Vesicle. 2022 December ; 1: . doi:10.1016/j.vesic.2022.100016.

Sucrose-based cryoprotective storage of extracellular vesicles

Sierra A. Walker[1,#], **Irina Davidovich**[2,#], **Yubo Yang**[1], **Andrew Lai**[3], **Jenifer Pendiuk Goncalves**[4,5], **Vatsal Deliwala**[4,5], **Sara Busatto**[6,7], **Shane Shapiro**[8], **Na'ama Koifman**[9], **Carlos Salomon**[3,10,*], **Yeshayahu Talmon**[2,*], **Joy Wolfram**[4,5,*]

[1]Department of Biochemistry and Molecular Biology, Department of Physiology and Biomedical Engineering, Department of Transplantation, Mayo Clinic, Jacksonville, FL 32224, USA

[2]Department of Chemical Engineering and the Russell Berrie Nanotechnology Institute (RBNI), Technion-Israel Institute of Technology, Haifa 3200003, Israel

[3]Exosome Biology Laboratory, Centre for Clinical Diagnostics, University of Queensland Centre for Clinical Research, Royal Brisbane and Women's Hospital, Faculty of Medicine, The University of Queensland, Brisbane, QLD 4006, Australia.

[4]Australian Institute for Bioengineering and Nanotechnology, The University of Queensland, Brisbane, QLD 4072, Australia

[5]School of Chemical Engineering, The University of Queensland, Brisbane, QLD, Australia

[6]Vascular Biology Program, Boston Children's Hospital, Boston, MA 02115, United States

[7]Department of Surgery, Harvard Medical School, Boston, MA 02115, United States

[8]Department of Orthopedic Surgery, Mayo Clinic, Jacksonville, FL 32224, USA

[9]Center of Microscopy and Microanalysis, The University of Queensland, Brisbane, QLD 4072, Australia

[10]Departamento de Investigación, Postgrado y Educación Continua (DIPEC), Facultad de Ciencias de la Salud, Universidad del Alba, Santiago 8320000, Chile

Abstract

Advancements in extracellular vesicle (EV) studies necessitate the development of optimized storage conditions to ensure preservation of physical and biochemical characteristics. In this study, the most common buffer for EV storage (phosphate-buffered saline/PBS) was compared to a cryoprotective 5% sucrose solution. The size distribution and concentration of EVs from two different sources changed to a greater extent after −80 °C storage in PBS compared to the

[*]Corresponding authors: c.salomongallo@uq.edu.au (CS); ishi@technion.ac.il (YT); j.wolfram@uq.edu.au (JW), The University of Queensland, Brisbane, QLD 4072, Australia.

Author contributions

This study was conceptualized by JW, YT, and YY. Extracellular vesicles were isolated by AL, SAW, SB, and YY. Data were collected by AL, ID, JPG, NK, SAW, and VD. Technical support was provided by JW, NK, SB, SS, CS, and YT. Supervision and funding were provided by CS, JW, and YT. All authors provided intellectual contributions to this work. SAW and JW wrote the manuscript, which was revised and approved by all authors.

[#]These authors contributed equally

Competing Interests

The authors declare that they have no competing interests.

sucrose solution. Additionally, molecular surface protrusions and transmembrane proteins were more prevalent in EVs stored in the sucrose solution compared to those stored in PBS. This study demonstrates, for the first time, that distinct ring-like molecular complexes and cristae-like folded membranous structures are visible upon EV degradation. Taken together, the size, concentration, molecular surface extensions, and transmembrane proteins of EVs varied substantially based on the buffer used for −80 °C storage, suggesting that biocompatible cryoprotectants, such as sucrose, should be considered for EV studies.

Keywords

Cryoprotection; exosome; extracellular vesicle; storage; sucrose

1. Introduction

Extracellular vesicles (EVs) are cell-released, lipid bilayer nanoparticles with protein,[1] nucleic acid,[2] lipid,[3] and carbohydrate cargo.[4] The use of EVs in mechanistic,[5] diagnostic,[6,7] and therapeutic[8–12] preclinical and clinical studies is rapidly growing, making storage an important consideration. Current convention for EV storage is freezing in phosphate-buffered saline (PBS) at −80 °C or −70 °C.[13,14] Storage at these conditions may be insufficient to prevent fusion, damage, and fragmentation of EVs, which could alter functional properties.[13] Lyophilization, which uses vacuum sublimation and desorption to remove water molecules from a sample, has also been explored as an alternative to storage at −80 °C.[15] In nano-drug carriers, such as liposomes, this can improve long-term stability, and circumvent expensive storage solutions.[16] However, bilayers may be destroyed in the freeze-drying process, vesicle fusion may occur during rehydration, and there is usually an overall reduction in particle numbers.[13] Temperature-dependent changes to physical parameters in EV samples call for the use of cryoprotectants. The two main categories of cryoprotectants are permeable (for example, glycerol, dimethylsulfoxide (DMSO), propanediol, and methanol) and non-permeable (for example, polyethylene glycol (PEG), polyvinyl alcohol, raffinose, trehalose, mannitol, glucose, and sucrose).[13,14] Some cryopreservation reagents, such as DMSO, could have cytotoxic effects if they remain in EV samples after storage.[13] Non-permeating cryoprotective agents, such as sucrose, that replace surrounding hydration spheres through hydrogen bonding interactions, represent a biocompatible alternative.

Sucrose has been used previously in therapeutic formulations for intravenous delivery up to a concentration of 19.5% (weight/volume), as approved by the United States Food and Drug Administration (FDA).[17,18] Notably, clinical-grade measles virus preparations, which have applications in vaccination and in oncolytic viral therapies, have remained stable for more than six years in 5% sucrose.[19,20] Measles viruses are of similar size and density as EVs, making sucrose a promising cryoprotective agent for EV storage.

In this study, the effects of a sucrose-based cryoprotectant were compared to those of PBS for EV storage at −80 °C. Specifically, a clinical-grade 5% sucrose buffer containing 50 mM tris(hydroxymethyl) aminomethane (Tris) and 2 mM $MgCl_2$ was assessed. In addition

to cryoprotection, the components of the buffer contribute to isotonicity and physiological pH. Size distribution profiles and concentrations of freshly collected and stored EVs were determined by nanoparticle tracking analysis. EV morphology and molecular surface extensions were visualized by cryogenic-transmission electron microscopy, while membrane protein levels were assessed by Western blotting.

2. Materials and Methods

2.1. Materials

Materials were acquired from the following sources: mouse secondary antibody (Cat. No. 31450), high performance liquid chromatography (HPLC)-grade water, SuperSignal West-Femto maximum sensitivity substrate (enhanced chemiluminescence, ECL), Pierce bicinchoninic acid assay (BCA) Protein Assay Kit, Tween 20, 3-N-morpholinopropanesulfonic acid (MOPS) buffer, and NuPAGE 12% Bis-Tris protein gels from Thermo Fisher Scientific (Waltham, MA, USA); fetal bovine serum (FBS), DMSO, and sodium hydroxide beads (20–40 mesh, Cat. No. 367176) from Sigma-Aldrich (St. Louis, MO, USA); clinical-grade sucrose buffer (5% sucrose, 50 mM Tris, and 2 mM $MgCl_2$, 08–735B) from Sartorius/Lonza (Bend, OR, USA); ultrapure sterile water from Rocky Mountain Biologicals (Missoula, MT, USA); nitrocellulose transfer membrane from Abcam (Cambridge, MA, USA); high glucose Dulbecco's modified Eagle's medium (DMEM) from Life Technologies, HyClone PBS from GE Healthcare (Chicago, IL, USA).

2.2. Cell culture

Human MDA-MB-231 breast cancer cells (HTB-26; ATCC) and human MeT-5A pleural mesothelial cells (CRL-9444; ATCC) were cultured and maintained in high-glucose Dulbecco's modified Eagle medium (DMEM, Life Technologies) or Roswell Park Memorial Institute (RPMI) 1640 Medium, respectively. Both media were supplemented with 10% FBS (Sigma), and 1% penicillin/streptomycin (Gemini Bioproducts) at 37 °C in 5% CO_2. Cells were used between passage numbers 5–20.

2.3. EV isolation

For EV isolation from MDA-MB-231 cells, cells were seeded in 150 mm dishes with DMEM, supplemented with 10% EV-depleted FBS (Exosome-depleted FBS; System Biosciences). The conditioned medium was collected after 48 hours, when the cells were 90% confluent and over 95% viable (Trypan blue). The same conditioned medium was used to prepare EVs stored in PBS or sucrose, to eliminate effects of cell culture conditions on EV characteristics. Conditioned cell culture medium was centrifuged (800 × g; 30 min; Sorvall ST 16R centrifuge, Thermo Scientific) to discard dead cells and large cellular debris. EVs were isolated using a KrosFlo Research 2i Tangential Flow Filtration (TFF) System (Spectrum Labs), as previously described.[21–25] Briefly, the supernatant of the conditioned cell culture medium (0.5–0.8 L) was filtered using a sterile hollow fiber modified polyethersulfone membrane with 0.65 μm (D02-E65U-07-S; Spectrum Labs) molecular weight cut-off pores and a polysulfone membrane with 500 kD (D02-S500–05-S; Spectrum Labs) molecular weight cut-off pores to remove any remaining cell debris and small biomolecules. Filters were washed with sterile PBS (pH 7.4; 3x volume of the filter)

prior to processing the conditioned medium. The input flow rate was 80 mL/min to keep the shear force below 2000/second. EVs were concentrated and diafiltrated six times in sterile PBS or the sterile sucrose solution (5% sucrose, 50 mM Tris, and 2 mM $MgCl_2$). Finally, EV samples were concentrated to 6–9 mL by TFF and stored at −80 °C.

For EV isolation from MeT-5A cells, cells were seeded into two T-175 flasks and cultured in RPMI 1640 containing FBS until ~70–80% confluent. At this point, cells were washed twice with PBS and cultured with RPMI 1640 without FBS. After 48 hours, the cell conditioned medium (40 mL) was centrifuged (300 × g; 5 min; Avanti J-15R centrifuge, Backman Coulter, Brea, CA, USA), filtered (0.45 μm; Cat. No. 431220; Corning, New York, USA) and concentrated to 0.5 mL by ultrafiltration with a Amicon Ultra-15 100 kDA molecular weight cutoff filter (Cat. No. UFC910008; Merck, Burlington, MA, USA). EVs were then isolated by size-exclusion chromatography (SEC) using qEVoriginal 70 nm columns (Izon, Christchurch, New Zealand). The collected EV fractions (1.5 mL) were divided into two and were concentrated and diafiltrated in sterile PBS or sucrose solution. EV samples were used immediately for downstream characterization or stored at −80 °C

2.4. Nanoparticle tracking analysis

A NanoSight NS300 (Software v3.3/3.4; Malvern Panalytical, Malvern, United Kingdom) was used to assess EV size distribution profiles and concentration. MDA-MB-231 EV samples diafiltered in PBS or a sucrose solution by TFF were diluted 1:50 in PBS and five one-minute videos were recorded using a camera level of 11 and a detection threshold of three. MeT-5A EV samples obtained through SEC were diluted 1:100 in 0.1 μm PBS and five 30-second videos were recorded using a camera level of 13 and a detection threshold of five. Each replicate was measured under a continuous syringe pump flow rate of 40 μL/min. Only the focus was changed between samples, not the analytical software parameters.

2.5. Zeta potential

Samples were diluted 1:50 in water and placed in folded capillary cells (Malvern, Malvern, United Kingdom; #DTS1070) and a Zetasizer nano series Nano-ZS by Malvern was used to measure the zeta potential. Material calculations are based on a refractive index (RI) of 1.370 and absorption of 0.010. Viscosity of the dispersant is 0.8872 cP with RI: 1.330 and dielectric constant of 78.5. The Smoluchowski model was used with F (ka) value of 1.5. Each sample had an equilibration time of 30 seconds, and each capture was for 20 runs.

2.6. BCA protein assay

A bicinchoninic acid (BCA) protein assay was performed to determine the protein concentration of each sample according to the manufacturer’s instructions.

2.7. Western blot

All samples were normalized to protein content. Sodium dodecylsulfate (6 X) was added to each sample at a 1:6 ratio, and samples were boiled for five minutes at 95 °C. The equivalent of 10.9 μg of protein were loaded in each well of a 12% polyacrylamide gel in MOPS buffer, and electrophoresis was performed for 1.5–2 hours at 120 V. Transfer from the gel to a nitrocellulose membrane was completed at 200 mA for 1.5 hours. The

membrane was blocked at room temperature with 5% milk in Tris-buffered saline (TBS) + 0.1% Tween (TBST) for two hours. Primary antibodies in 1% milk in TBST (1:500 dilution) were incubated overnight at 4 °C. The following primary antibodies were used: anti-calnexin (#ab22595; Abcam, Waltham MA, USA), anti-CD63 (#ab134045; Abcam, Waltham, MA, USA), anti-annexin V (#ab14196; Abcam, Waltham, MA, USA), and anti-CD81 (#sc-166029; Santa Cruz, Dallas, TX, USA). Secondary antibodies (anti-rabbit and anti-mouse, #7074S and #7076S, respectively) were both purchased from Cell Signaling (Danvers, MA, USA). After four five-minute washes with TBST, secondary antibody in 1% milk in TBST (1:3000 dilution) were incubated for two hours at room temperature, before four final five-minute washes with TBST and developing the membrane in an ECL solution for five minutes at room temperature in the dark. Images were collected using an Amersham 600 imager (GE Healthcare, Chicago, IL, USA).

2.8. Volta phase-plate cryogenic-transmission electron microscopy (cryo-TEM)

A drop (~3 μL) of EV dispersion (10^{10}/mL) was placed within a controlled environment vitrification system (CEVS) on a perforated carbon film, supported on a 200 mesh TEM grid, mounted on a tweezer, as previously described.[26–28] The drop was turned into a thin liquid film (preferably less than 300 nm) by blotting away the excess solution with filter paper mounted on a metal strip. The grid was then quickly plunged into freezing ethane (−183 °C), and imaged in an FEI (now Thermo Fisher Scientific) Talos 200C high-resolution TEM, at −180 °C. The Volta phase-plate was used to enhance image contrast. The images were acquired at an acceleration voltage of 200 kV and recorded by an FEI Falcon III direct-imaging camera under low electron exposure.

2.9. 300 kV cryo-TEM

Specimens of EVs from MeT-5A cells were prepared in a robotic vitrification system, Leica EM GP2, at controlled temperature and humidity of 22 °C and 95%, respectively. An EV dispersion (2 μL) was placed on a QuantifoilTM carbon film with circular holes of 3.5 μm diameter and an interspace of 1 μm in both dimensions, supported on a 200-mesh copper grid. The excess solution was automatically blotted for 2–2.5 seconds and rapidly plunged into liquid ethane close to its freezing point (−182.8 °C). Grids were then quickly transferred into liquid nitrogen for storage. Samples were imaged in a frozen hydrated state at −176°C using a JEOL Cryo ARM 300 (JEM-Z300FSC) TEM, equipped with a cold field emission gun (FEG), and an in-column Omega energy filter. Zero energy loss images were acquired at an acceleration voltage of 300 kV and a filter setting of 20 eV. Images were recorded by a Gatan K3 direct detector camera under low-dose exposure conditions using SerialEM* software.[29]

3. Results and discussion

In this study, the size, concentration, and zeta potential of cell-culture derived EVs stored in PBS or a 5% sucrose solution (with 50 mM Tris and 2 mM $MgCl_2$) at −80 °C were compared. EVs were isolated by TFF, which provides gentle and controlled size-dependent separation that is scalable to large volumes and results in high batch-to-batch consistency and purity.[21] EVs were also isolated by SEC, which similarly provides gentle and size-

dependent separation of EVs, and is ideal for smaller volumes.[4] Other common EV isolation methods, such as ultracentrifugation, are known to impair EV integrity,[30] making them less ideal for assessing additional storage-induced damage. The results demonstrated that TFF-isolated EVs stored at −80 °C in a sucrose solution had improved stability over a 15-week period compared to ones stored in PBS. Specifically, nanoparticle tracking analysis demonstrated that PBS storage resulted in more substantial changes in EV size distribution profiles (Figure 1a) compared to sucrose storage (Figure 1c), although both caused the peak population to decrease in size. For both fresh and frozen samples, the smallest detectable particle size was 60 nm (Figures 1a and 1c), which corresponds to the estimated lower limit of detection of nanoparticle tracking analysis (60–70 nm).[31] Additionally, PBS storage resulted in a statistically significant increase in EV concentrations at all time points (Figure 1b), while the EV concentration remained unchanged following storage in the sucrose solution, except for the 15-week time point when the concentration decreased (Figure 1d). Storage at −80 °C in PBS or the sucrose solution did not cause a statistically significant change in EV zeta potential (Figure 1e).

To more broadly assess the effects of sucrose-based cryoprotection, a different EV source (human MeT-5A pleural mesothelial cells) and isolation method (SEC) were assessed. Similar results were obtained as those for MDA-MB-231 EVs isolated by TFF, where EV characteristics changed to a greater extent after −80 °C storage in PBS compared to the sucrose solution (Figure 2). Specifically, the PBS group displayed a more statistically significant shift in EV size distribution between fresh and frozen samples compared to the sucrose group, and storage caused the peak population to decrease in size in both groups (Figure 2a and 2c). Additionally, −80 °C storage of EVs in PBS caused a statistically significant reduction in EV concentration (Figure 2b), while the concentration remained unchanged in sucrose (Figure 2d). On the contrary to the MDA-MB-231 EVs, storage caused a statistically significant decrease and increase in the zeta potential of EVs stored in PBS and sucrose, respectively (Figure 1e). It is likely that changes in the size, concentration, and zeta potential of stored EVs are driven by freezing and thawing-induced alterations in membrane structures.[13] For example, a size decrease and concentration increase as seen with the MDA-MB-231 EV samples stored in PBS, may be indicative of EV fragmentation, while a size decrease and concentration decrease as seen with MeT-5A EV samples stored in PBS may be indicative of EV degradation (Figure 3) or fragmentation below the detectable size threshold.

High-contrast Volta phase-plate cryogenic TEM was used to assess the morphology and surface structure of TFF-isolated EVs stored in PBS or the sucrose solution at −80 °C. The results showed that molecular surface protrusions were more prevalent in samples stored in the sucrose solution than in PBS (Figure 4a and 4b). Similar membrane protrusions have previously been visualized on freshly prepared MDA-MB-231-derived EVs, in which case they were hypothesized to be glycoproteins.[32] Further studies are necessary to fully determine the molecular nature of these protrusions, which are also likely to vary depending on the EV type and source. In fact, fresh MeT-5A-derived EVs lacked surface protrusions (Supplementary Figure 1), making it more challenging to determine potential storage-induced damage. Cryo-TEM also revealed the presence of multilamellar EV structures

(Figure 4a), which can occur during the freezing process as ice crystals disrupt lipid membranes.[33]

Additionally, Western blot analysis demonstrated that the transmembrane proteins, CD63 and CD81, which are common EV markers, were enriched in samples stored in a sucrose solution compared to those stored in PBS. Specifically, expression levels of CD63 and CD81 were calculated based on relative expression to the cytosolic EV protein, annexin V, and normalized to the PBS samples, demonstrating a 1.7-fold increase in both transmembrane proteins in the sucrose samples (Figure 4c).

Previous studies have found that EV proteins shift from higher molecular weights to lower molecular weights upon storage in PBS at 4 °C and −80 °C, indicating that degradation occurs.[33] It is likely that freezing and thawing in PBS also causes proteins to degrade and/or disassociate from the EV surface.[13,33] In particular, membrane proteins have been shown to decrease in concentration,[13] as well as undergo irreversible conformational changes[34] as a function of the rate of cooling or rewarming, changes in osmotic pressure, and generation of ice crystals.[13] The results from this study are in line with previous observations of EV storage in PBS, and indicate that a sucrose solution can be used as a better alternative to preserve surface molecules.

Studies were also performed to assess EV degradation upon room temperature storage for four days in the sucrose solution. Cryogenic-TEM images showed, for the first time, that EV samples in sucrose degrade into distinct ring-like biomolecular structures (~10 nm) (Figure 5a and 5b) and cristae-like folded membranous structures (~25 nm) (Figure 5c). Sucrose may be essential in the structural preservation of degradation products, and further studies will be necessary to characterize such products as well as degradation kinetics.

4. Conclusions

The use cryoprotective agents for EV storage is not a standard practice.[13] This study demonstrates that several physical and biomolecular features of EVs change upon storage in PBS at −80 °C, which should be taken into consideration for both preclinical and clinical EV studies. The cryoprotective properties of a 5% sucrose solution (with 50 mM Tris, and 2 mM $MgCl_2$) were assessed and compared to PBS storage. Storage at −80 °C in the sucrose solution outperformed PBS in terms of preserving EV size distribution profiles, concentration, biomolecular surface protrusions, and membrane proteins. Additional studies will be necessary to broadly assess the effects of this sucrose buffer in terms of other EV types and isolation methods. The results of this study support previously reported observations for the storage of measles virus, where a sucrose solution protects membrane structures.[17–20] A 5% sucrose concentration is below the amount approved by the FDA in the United States for intravenous administration (19.5%).[17,18] Further studies will be necessary to address the potential impact of sucrose on mechanistic, diagnostic, and therapeutic uses of EVs.

Supplementary Material

Refer to Web version on PubMed Central for supplementary material.

Acknowledgements

This work is partially supported by the Mayo Clinic Center for Regenerative Medicine in Florida, United States (JW), the Mayo Clinic Center for Biomedical Discovery, United States (JW), National Institute of Allergy and Infectious Diseases, National Institutes of Health (NIH), United States under award numbers R21AI152318 (JW), the American Heart Association, United States under award number 20TPA35490415 (JW), the Mayo Clinic Eagles Cancer Telethon, United States (JW), the Louis V. Gerstner Jr. Fund at Vanguard Charitable, United States (SS), The Israel Science Foundation, Israel under award number #2302/20 (YT), the China Scholarship Council, China (YY), the Medical Research Future Fund, Australia under award number MRF1199984 (CS), the National Health and Medical Research Council, Australia under award number NHMRC 1195451 (CS), and the University of Queensland (JW). The cryo-TEM work was performed at the Technion Center for Electron Microscopy of Soft Matter and at The University of Queensland Center of Microscopy and Microanalysis. The content is solely the responsibility of the authors and does not necessarily represent the official views of the funding agencies.

References

1. Bastos-Amador P et al. Proteomic analysis of microvesicles from plasma of healthy donors reveals high individual variability. J. Proteomics 75, 3574–3584, doi:10.1016/j.jprot.2012.03.054 (2012). [PubMed: 22516433]
2. Hunter MP et al. Detection of microRNA expression in human peripheral blood microvesicles. PLoS One 3, e3694, doi:10.1371/journal.pone.0003694 (2008). [PubMed: 19002258]
3. Chen S et al. Lipidomic characterization of extracellular vesicles in human serum. J Circ Biomark 8, 1849454419879848, doi:10.1177/1849454419879848 (2019).
4. Walker SA et al. Glycan Node Analysis of Plasma-Derived Extracellular Vesicles. Cells 9, 1946, doi:10.3390/cells9091946 (2020). [PubMed: 32842648]
5. van Niel G, D'Angelo G & Raposo G Shedding light on the cell biology of extracellular vesicles. Nat. Rev. Mol. Cell Biol 19, 213–228, doi:10.1038/nrm.2017.125 (2018). [PubMed: 29339798]
6. Hu T, Wolfram J & Srivastava S Extracellular Vesicles in Cancer Detection: Hopes and Hypes. Trends Cancer, doi:10.1016/j.trecan.2020.09.003 (2020).
7. Roy S, Hochberg FH & Jones PS Extracellular vesicles: the growth as diagnostics and therapeutics; a survey. J Extracell Vesicles 7, 1438720, doi:10.1080/20013078.2018.1438720 (2018). [PubMed: 29511461]
8. Witwer KW & Wolfram J Extracellular vesicles versus synthetic nanoparticles for drug delivery. Nature Reviews Materials 6, 103–106, doi:10.1038/s41578-020-00277-6 (2021).
9. Busatto S, Pham A, Suh A, Shapiro S & Wolfram J Organotropic drug delivery: Synthetic nanoparticles and extracellular vesicles. Biomed. Microdevices 21, 46, doi:10.1007/s10544-019-0396-7 (2019). [PubMed: 30989386]
10. Suh A et al. Adipose-derived cellular and cell-derived regenerative therapies in dermatology and aesthetic rejuvenation. Ageing Res Rev 54, 100933, doi:10.1016/j.arr.2019.100933 (2019). [PubMed: 31247326]
11. Ali M, Pham A, Wang X, Wolfram J & Pham S Extracellular vesicles for treatment of solid organ ischemia-reperfusion injury. Am. J. Transplant, doi:10.1111/ajt.16164 (2020).
12. Iannotta D, Yang M, Celia C, Di Marzio L & Wolfram J Extracellular vesicle therapeutics from plasma and adipose tissue. Nano Today 39, 101159, doi:10.1016/j.nantod.2021.101159 (2021). [PubMed: 33968157]
13. Qin B et al. How does temperature play a role in the storage of extracellular vesicles? J Cell Physiol 235, 7663–7680, doi:10.1002/jcp.29700 (2020). [PubMed: 32324279]
14. Kusuma GD et al. To Protect and to Preserve: Novel Preservation Strategies for Extracellular Vesicles. Front. Pharmacol 9, 1199, doi:10.3389/fphar.2018.01199 (2018). [PubMed: 30420804]
15. Charoenviriyakul C, Takahashi Y, Nishikawa M & Takakura Y Preservation of exosomes at room temperature using lyophilization. Int J Pharm 553, 1–7, doi:10.1016/j.ijpharm.2018.10.032 (2018). [PubMed: 30316791]
16. El-Nesr OH, Yahiya SA & El-Gazayerly ON Effect of formulation design and freeze-drying on properties of fluconazole multilamellar liposomes. Saudi Pharm J 18, 217–224, doi:10.1016/j.jsps.2010.07.003 (2010). [PubMed: 23960730]

17. Frankenfeld C et al. Daptomycin: a comparison of two intravenous formulations. Drug Des Devel Ther 12, 1953–1958, doi:10.2147/DDDT.S167010 (2018).
18. FDA. Database of Inactive Ingredient for Approved Drug Products, <https://www.accessdata.fda.gov/scripts/cder/iig/index.cfm> (2021).
19. Ungerechts G et al. Moving oncolytic viruses into the clinic: clinical-grade production, purification, and characterization of diverse oncolytic viruses. Mol Ther Methods Clin Dev 3, 16018, doi:10.1038/mtm.2016.18 (2016). [PubMed: 27088104]
20. Langfield KK, Walker HJ, Gregory LC & Federspiel MJ Manufacture of measles viruses. Methods Mol. Biol 737, 345–366, doi:10.1007/978-1-61779-095-9_14 (2011). [PubMed: 21590404]
21. Busatto S et al. Tangential Flow Filtration for Highly Efficient Concentration of Extracellular Vesicles from Large Volumes of Fluid. Cells 7, 273, doi:10.3390/cells7120273 (2018). [PubMed: 30558352]
22. Tian M et al. Adipose-Derived Biogenic Nanoparticles for Suppression of Inflammation. Small 16, e1904064, doi:10.1002/smll.201904064 (2020). [PubMed: 32067382]
23. Busatto S et al. Brain metastases-derived extracellular vesicles induce binding and aggregation of low-density lipoprotein. J Nanobiotechnology 18, 162, doi:10.1186/s12951-020-00722-2 (2020). [PubMed: 33160390]
24. Busatto S, Iannotta D, Walker SA, Di Marzio L & Wolfram J A Simple and Quick Method for Loading Proteins in Extracellular Vesicles. Pharmaceuticals (Basel) 14, 356, doi:10.3390/ph14040356 (2021). [PubMed: 33924377]
25. Wang X et al. Effects of Adipose-Derived Biogenic Nanoparticle-Associated microRNA-451a on Toll-like Receptor 4-Induced Cytokines. Pharmaceutics 14, doi:10.3390/pharmaceutics14010016 (2021).
26. Koifman N, Biran I, Aharon A, Brenner B & Talmon Y A direct-imaging cryo-EM study of shedding extracellular vesicles from leukemic monocytes. J Struct Biol 198, 177–185, doi:10.1016/j.jsb.2017.02.004 (2017). [PubMed: 28254382]
27. Busatto S et al. Considerations for extracellular vesicle and lipoprotein interactions in cell culture assays. J Extracell Vesicles 11, e12202, doi:10.1002/jev2.12202 (2022). [PubMed: 35362268]
28. Yang M et al. Extracellular vesicle glucose transporter-1 and glycan features in monocyte-endothelial inflammatory interactions. Nanomedicine, 102515, doi:10.1016/j.nano.2022.102515 (2022). [PubMed: 35074500]
29. Mastronarde DN Automated electron microscope tomography using robust prediction of specimen movements. J. Struct. Biol 152, 36–51, doi:10.1016/j.jsb.2005.07.007 (2005). [PubMed: 16182563]
30. Coumans FAW et al. Methodological Guidelines to Study Extracellular Vesicles. Circ. Res 120, 1632–1648, doi:10.1161/CIRCRESAHA.117.309417 (2017). [PubMed: 28495994]
31. Bachurski D et al. Extracellular vesicle measurements with nanoparticle tracking analysis - An accuracy and repeatability comparison between NanoSight NS300 and ZetaView. J Extracell Vesicles 8, 1596016, doi:10.1080/20013078.2019.1596016 (2019). [PubMed: 30988894]
32. Issman L, Brenner B, Talmon Y & Aharon A Cryogenic transmission electron microscopy nanostructural study of shed microparticles. PLoS One 8, e83680, doi:10.1371/journal.pone.0083680 (2013). [PubMed: 24386253]
33. Maroto R et al. Effects of storage temperature on airway exosome integrity for diagnostic and functional analyses. J Extracell Vesicles 6, 1359478, doi:10.1080/20013078.2017.1359478 (2017). [PubMed: 28819550]
34. Nardid O, Dyubko T & Repina S A comparative study of the effect of freeze-thawing on peripheral and integral membrane proteins. Cryobiology 34, 107–113, doi:10.1006/cryo.1996.1986 (1997). [PubMed: 9130383]

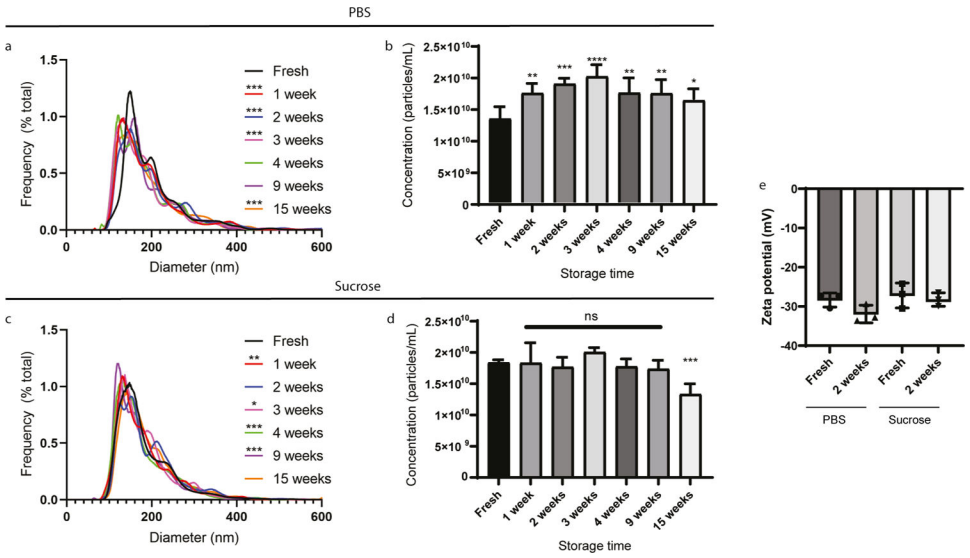

Figure 1. Size and concentration of MDA-MB-231 cell-derived extracellular vesicles (EVs) stored in phosphate-buffered saline (PBS) or a 5% sucrose solution at −80 °C.

Nanoparticle tracking analysis measurements were performed on EVs in PBS (a and b) or sucrose solution (c and d). a,c) Size distribution of EVs as percent frequency in 1 nm increments. b,d) Concentration of EVs. Data represent mean + standard error of mean (SEM) of five technical replicates. e) Zeta potential of MDA-MB-231 cell-derived EVs. Data represent mean +/− standard deviation (SD) of triplicates. Statistics by Friedman's test with Dunn's multiple comparison correction (a, c) or analysis of variance (ANOVA) followed by Dunnett correction (b, d) or ANOVA followed by Tukey's correction (e). *, $p < 0.05$; **, $p < 0.01$; ***, $p < 0.001$; ****, $p < 0.0001$; ns, not significant.

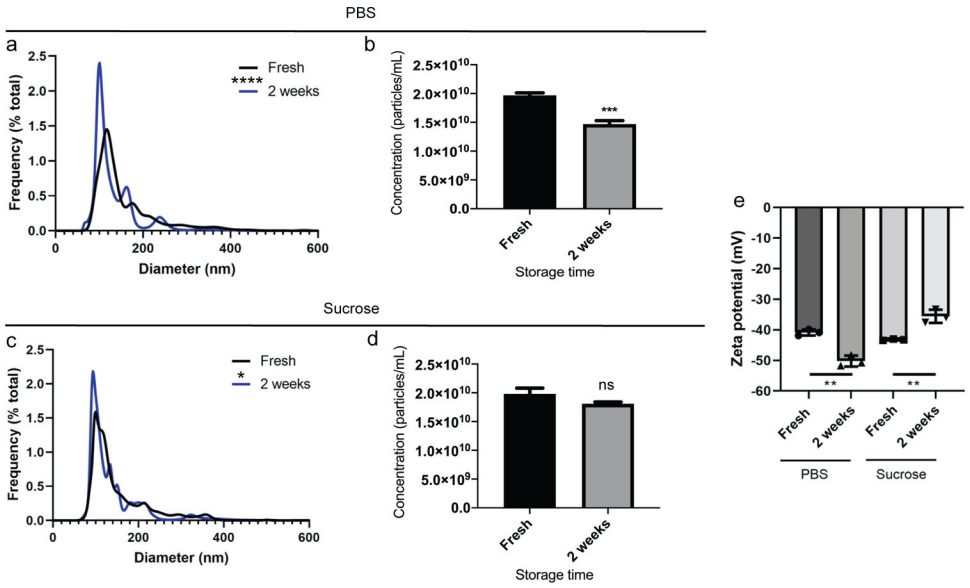

Figure 2. Size, concentration and zeta potential of MeT-5A cell-derived EVs stored in PBS or a 5% sucrose solution at −80 °C.

Nanoparticle tracking analysis measurements were performed on EVs in PBS (a and b) or sucrose solution (c and d). a, c) Size distribution of EVs as percent frequency in 1 nm increments. b,d) Concentration of EVs. Data represent mean + standard error of mean (SEM) of five technical replicates. e) Zeta potential of EVs. Data represent mean +/− standard deviation (SD) of triplicates. Statistics by Wilcoxon matched-pairs signed rank test (a, c), *t*-test with Welch's correction (b, d), or ANOVA followed by Tukey's multiple comparisons test (e). *, $p < 0.05$; ***, $p < 0.001$; ****, $p < 0.0001$.

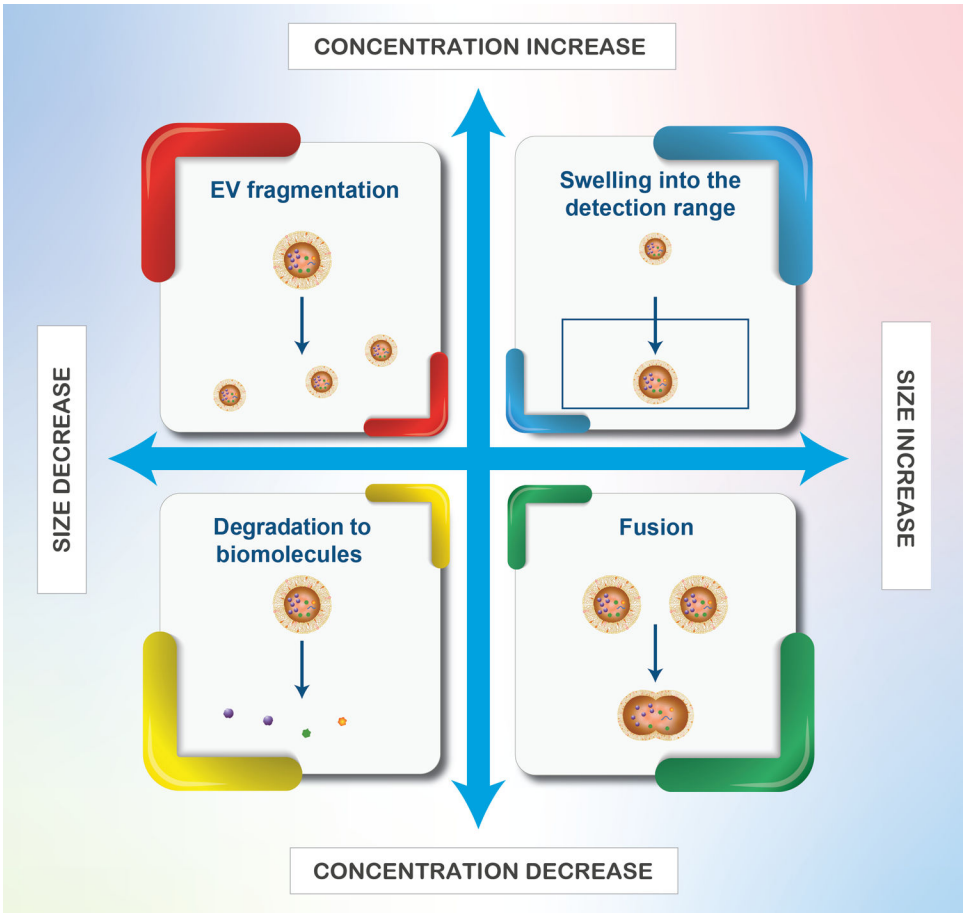

Figure 3. Tandem size and concentration changes during, freezing, storage, and thawing of EVs.
Fragmentation may also lead to EVs with open membranes (not shown above).

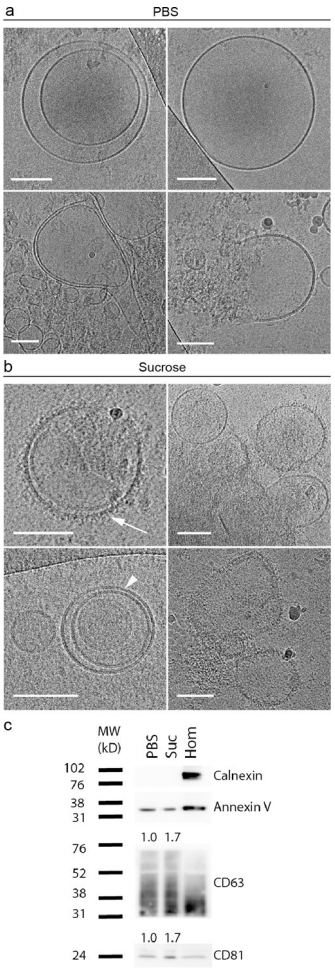

Figure 4. Morphology and protein markers on EVs (MDA-MB-231 cell-derived) stored in PBS or a 5% sucrose solution (Suc) at −80 °C.

a,b) Cryogenic transmission electron microscopy (cryo-TEM) images. Scale bars correspond to 100 nm. Arrowhead: lipid bilayer resolved into its two leaflets; arrow: surface protrusions. c) Western blot analysis of calnexin (intracellular contaminant marker), cluster of differentiation (CD) markers CD63 and CD81 (transmembrane EV markers), and annexin V (cytosolic EV marker). Hom, cell homogenate control. Levels of transmembrane proteins CD63 and CD81 were calculated based on relative expression to the cytosolic protein, annexin V, and normalized to the PBS group; quantified values are reported above the protein bands.

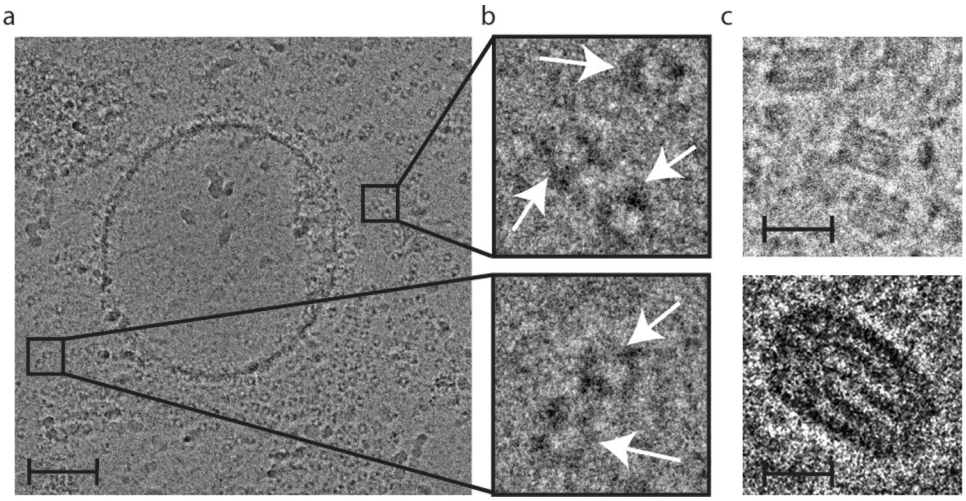

Figure 5. Morphology of EVs (MDA-MB-231 cell-derived) stored in a 5% sucrose solution at room temperature for four days.

a) Cryo-TEM image demonstrative of vesicle degradation into ring-like structures. Scale bar, 100 nm. b) Insets of (a) with arrows indicating ring-like structures. Inset widths, 50 nm. c) Cristae-like membranous structures. Scale bars, 25 nm (upper) and 10 nm (lower).